Effects of Polymer Adsorption and Grafting on Entanglements and Dynamics of Model Polymer Nanocomposites

Background

Effect of Polymer Adsorption

It is well known that the addition of nanoparticle (NP) fillers in polymer matrices can alter the mechanical strength and viscoelastic properties of polymers. Thus, the application of these materials is significant due to improvements in optical, electrical, and thermomechanical properties.[1-4] One major application is that nanoparticle fillers such as carbon black and silica are a key component of tire tread compounds, as shown in Figure 1. These fillers are known to control the mechanical properties, particularly hysteresis, which plays a major role in traction, rolling resistance, and tire wear performance.[5-9] The type of ordering, interparticle spacing, and resulting material properties depend on many parameters that can be experimentally controlled such as particle surface chemistry, particle loading, the type and amount of coupling agent added (if any), and polymer chemistry.[10-12] However, the number of adjustable composition and processing parameters makes rational design of optimized materials impossible without a clear understanding of the underlying chemistry and physics of the system. Therefore, a major goal of this proposal is to understand how to tune mechanical properties in polymer nanocomposites, facilitating the design of materials with, for instance, high hysteresis in the operating conditions of traction and low hysteresis in the operating conditions of rolling resistance.

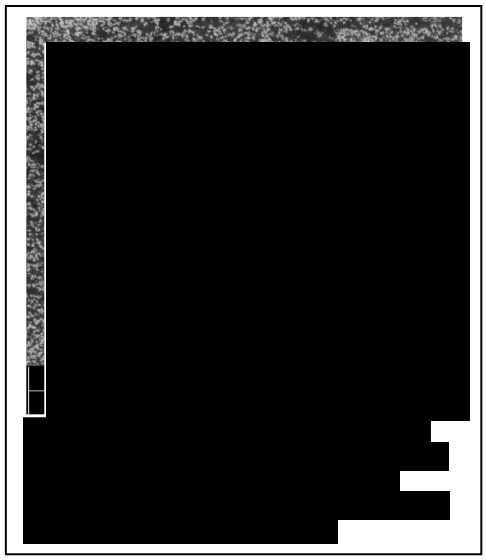

A crucial mechanism of hysteresis is the process of macromolecular desorption from and re-adsorption to filler surfaces.[13,14] Many factors are involved in setting how the polymer adsorbs, including the polymer length, stiffness, and especially the local polymer-particle chemical interactions.[14] The adsorption and thus the nanocomposite structure and dynamics can be experimentally controlled by modifying the particle surface chemistry (depending on particle type), using surface functional groups or coupling agents, or by using chemically different polymers.[15-20] This allows some control over the relaxation times, especially of adsorbed polymers, in different operating regimes. These relaxation times affect hysteresis, since hysteresis is maximized if the relaxation times are close to the reciprocal of the loading frequency. Hysteresis is also tunable by varying the nanoparticle loading fraction, which affects the number of atoms participating in the adsorption-desorption process, as well as the local strain between nanoparticles upon macroscopic loading.

Many prior simulation and theoretical studies on nanocomposites have yielded considerable progress in understanding the dynamics and conformational changes of polymers near the surface of nanoparticles.[10,12,14,21-34] Several groups have used molecular dynamics (MD) simulations to study the nanocomposite dynamic properties. More specifically, the viscosity, dynamic shear modulus,[35] and stress autocorrelation function (the Fourier transform of which

yields the storage and loss moduli as a function of frequency)[36] have been calculated from equilibrium simulations. Furthermore, non-equilibrium MD using the SLLOD equations of motion has been used to calculate viscosity as a function of shear rate, among other quantities.[22,37] A clear picture has developed that polymer-nanoparticle adsorption greatly affects nanocomposite dynamics, and adsorbed polymers have different (slower) relaxation than those in the bulk. Analytical theories can be used to predict the overall composite properties based on the amount of nanoparticles, adsorbed polymer properties, and amount of adsorbed layer.[38,39]

Effect of Grafting and Nanoparticle Arrangement

A common challenge in achieving enhanced properties for polymer nanocomposites (PNCs) is the ability to control the dispersion of the nanoparticles in the polymer matrix. Many studies have shown that grafting polymers to the nanoparticle, changing nanoparticle size, and altering the molecular weights of the grafted and free polymer can maximize the dispersion of NPs in a polymer blend.[40-46] More specifically, the curvature of the nanoparticle as well as interactions between the grafted polymer (brush) and matrix polymer affect the spatial organization of NPs.[43] Because NP interactions have an effect on NP dispersion, it is clear that grafting density exhibits a significant role in NP dispersion as well.[40-46] For example, at low grafting densities the morphology of PNCs can show aggregation due to attractive interactions between the NP cores, which compete with the interactions with the grafted polymer chains.[43] Meanwhile, the steric hindrance of polymers at higher grafting density prevents the nanoparticle-nanoparticle cores from interacting directly. However, when grafting density is too high, the matrix polymer cannot penetrate through the brush layer and dewetting occurs.[46]

From the previous studies on polymer grafted nanoparticles (PGNs), it is quite clear why understanding the properties of these nanocomposites is essential. The physical insight gained from MD simulations can suggest design rules for the development of new materials. There are still many questions to be answered for PGN systems. For example, how do grafted polymers in the entangled regime affect the mechanical and viscoelastic properties of the melt? How does the arrangement of nanoparticles in random versus close packed structures (that can form for systems with little free polymer) affect the entanglements and dynamics? What systems can give optimal amounts of entanglements? These are some of the key motivating questions to be investigated in this portion of the proposed work.

Overview of Proposed Work

The proposed work is to perform, validate, and analyze coarse-grained molecular dynamics simulations of model polymer nanocomposite (PNC) systems. In different parts of the work, polymer adsorption on a single particle and the effects of high particle loading and polymer grafting will be studied. In the adsorption study, copolymer systems will be studied in which one of the two types of monomers in the polymer adsorbs more strongly than the other; different polymer architectures will be investigated, ranging from two long blocks of the different monomer types in each chain to alternating types of monomers along the chain. The strength of the interaction potentials between the polymer and nanoparticle are the most important parameters needed to describe different chemical systems, and comparisons to experimental homopolymer systems can be used to choose appropriate values. The unlike monomer-monomer interactions are the only additional adjustable parameter to be validated

versus experimental copolymer systems. The simplified model, described further below, allows us to reach the time and length scales of interest to equilibrate the polymer around the particle or particles to determine equilibrium polymer conformations as well as relaxation times and certain mechanical properties. In particular, the first set of simulations will focus on relatively short copolymers and the dilute particle regime; this will allow us to equilibrate more quickly and to measure and analyze various properties locally as a function of distance from the nanoparticle surface.

Another set of simulations will study systems with only one type of monomer and nanoparticles that are either bare or decorated with polymer grafts. Both lightly entangled and highly entangled chains will be studied for un-grafted and grafted nanoparticles arranged at low to high packing fractions randomly or in a face-centered cubic (FCC) structure. The un-grafted PNC system will be used for comparison with the grafted and pure melt systems to see the effect of NP arrangement and grafting on polymer dynamics.

We will use a variety of methods to perform dynamic, mechanical, and rheological analysis on our simulated systems. Fluctuation dissipation relationships will be implemented to analyze dynamic properties from equilibrium systems. In addition, we will apply direct oscillatory shear at several frequencies for a subset of the systems. In collaboration with Kurt Koelling's group at OSU and Cooper Tire and Rubber Company, we have access to preliminary rheological data for systems of various amounts of silica particles dispersed in polystyrene, and we expect that further data for polystyrene-polybutadiene copolymers will be available in the coming 1-2 years. Agreement between simulated and experimental properties is desired, therefore we will use the results of these analyses to help validate and refine our simulations and understand the physical basis of experimental results.

Simulation Models

MD simulations including nanoparticles and polymer (free or grafted) are inherently difficult to equilibrate. Reaching the time and length scales required for particles to rearrange in such simulations would be very expensive or completely intractable for realistic particle sizes. Nanoparticle fillers can have structure on length scales exceeding 100 nanometers, and relaxations can occur on a length scale of micrometers and a time scale of milliseconds. On the other hand, atomistic motions occur on a length scale of angstroms and a timescale of femtoseconds.[23] We will use a coarse-grained freely jointed chain model as an efficient and relatively simple way to properly address molecular connectivity and structure without atomistic chemical detail; such a model has been used for polymer systems with various types of nanoparticles.[22,28,31] Specifically, our model is similar to the bead-spring model used by Kremer and Grest.[47]

Model and simulation details

Monomers and nanoparticles are modeled as spherical beads of different sizes. An example snapshot is shown in Figure 2 of a preliminary simulation with particles arranged in an FCC manner with periodic boundary conditions. (Such a configuration is relevant to polymer-grafted particles at high packing fractions to be discussed later; here it was chosen for testing and comparison to the random particle configurations.) Linear chains of length N are created using finitely extensible nonlinear elastic (FENE) spring potentials between adjacent beads,

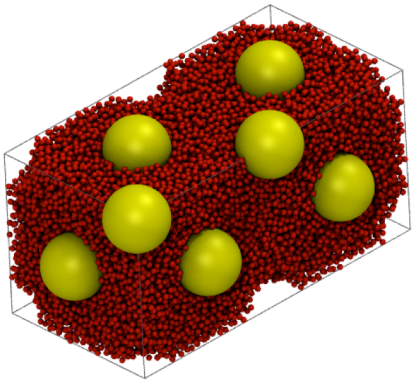

Figure 2. Snapshot of a polymer melt containing spherical nanoparticles arranged in an FCC structure.

$$U_{ij}^{\mathrm{FENE}} = \begin{cases} -\frac{1}{2}kR_0^2 \ln\left[1-\left(\frac{r_{ij}}{R_0}\right)^2\right], & r_{ij} \le R_0 \\ 0, & r_{ij} > R_0 \end{cases} \qquad (1)$$

where r_{ij} is the distance between particle bead i and j and R_0 is the maximum extent of the bond. The same FENE bonds are also used for grafted chains, except that the first bead is fixed on the particle surface. The constants k and R_0 are 30 and 1.5σ respectively, which prevents the beads from overlapping or breaking apart.[47] Monomer-monomer interactions follow a repulsive Lennard-Jones (LJ) potential, also known as the Weeks-Chandler-Anderson (WCA) potential,[48]

$$U_{ij}^{\mathrm{LJ}} = \begin{cases} 4\varepsilon\left[\left(\frac{\sigma}{r_{ij}}\right)^{12} - \left(\frac{\sigma}{r_{ij}}\right)^{6} + \frac{1}{4}\right], & r_{ij} \le r_c \\ 0, & r_{ij} > r_c \end{cases} \qquad (2)$$

where ε is the interaction energy and the cutoff radius r_c is set to $2^{1/6}\sigma$. The size and mass units of the simulation are the size and mass of single monomers ($\sigma = m = 1$). For homopolymer systems and preliminary copolymer work, all monomer-monomer interactions have $\varepsilon = 1$, in units of the thermal energy, though for copolymer system the cross interaction could be increased to account for unfavorable chemical interactions. Nanoparticle-nanoparticle interactions are represented using a shifted LJ potential,

$$U_{ij}^{\mathrm{LJshift}} = \begin{cases} 4\varepsilon\left[\left(\frac{\sigma}{r_{ij}-\Delta}\right)^{12} - \left(\frac{\sigma}{r_{ij}-\Delta}\right)^{6}\right], & r_{ij} \le r_c + \Delta \\ 0, & r_{ij} > r_c + \Delta \end{cases} \qquad (3)$$

where the shift factor $\Delta=(\sigma_{NP}-\sigma)$ in terms of the effective particle diameter σ_{NP}, as σ is the approximate range of the interaction before shifting. For fully repulsive systems (as in our study of high loading of grafted or bare nanoparticles in a homopolymers), nanoparticles also interact with the monomers through a shifted LJ potential with $\Delta=(\sigma_{NP}-\sigma)/2$. In the preliminary work, to represent the nanoparticles as spheres of diameter $\sigma_{NP} = 10\sigma$, Δ is set to 4.5. Particle mass is adjusted to account for their greater size using $m_p = 0.85\pi\sigma_{NP}^3/6$ (0.85 is approximately the melt density of the monomers).

The simulations are run using the large-scale atomic/molecular massively parallel simulator (LAMMPS) package.[67] After a brief pushoff using soft potentials to ensure no monomer overlaps remain from the initial randomly created configuration, each simulation is run first in an isobaric-isothermal ensemble using a Nosé-Hoover barostat and thermostat. The equations of motion used in the isobaric-isothermal ensemble are those of Shinoda et al.[57] For entangled chains, a bond-swapping algorithm can be used to allow chains to cross while equilibrating (as in our preliminary work at $N = 500$).[58] Once systems are fully equilibrated with

respect to polymer conformations, the systems are run in the NVT ensemble for data collection; for the preliminary work with FCC particles, for $N = 100$, or $5\text{x}10^6\ \tau$, and 6 x $10^5\ \tau$ for $N = 500$, where τ is the dimensionless LJ unit of time and each timestep is 0.01 τ.

Monomer-nanoparticle interaction for adsorption study

While many groups have studied coarse-grained models of polymer nanocomposites, a specific body of prior work that described the structure of the nanocomposite and the adsorbed polymer layer used a very simple model with a single chemical interaction parameter, ε_{NP}, which is of special interest here.[50-55] This parameter represents the enthalpic gain of a monomer coming into contact with the nanoparticle versus its reference state in the particle-free polymer solution. Specifically, the Polymer Reference Interaction Site Model (PRISM) liquid state theory was used to study the structure of polymer nanocomposites as a function of this parameter. Polymers were modeled as freely jointed chains of hard core monomers, and the particle-particle interactions were also purely hard core. The monomer-particle interactions were modeled as hard cores with an exponential attraction:

$$U_{NP}(r) = \begin{cases} \infty & ; \quad r < r_c \\ -\varepsilon_{NP} e^{-(r-r_c)/\alpha} & ; \quad r \geq r_c \end{cases}$$

The range of the attraction α was set at half of a monomer diameter, leaving the contact strength ε_{NP} as the single adjustable parameter. With ε_{NP} = 0.55 (in units of the thermal energy), the model reproduces the experimental scattering behavior of a silica-polyethylene oxide (PEO) system.[15] Experimental results of silica particles in polytetrahydrofuran (PTHF), which adsorbs on silica less strongly, could be reproduced by PRISM results at a lower ε_{NP}, which could be predicted from the difference in the chemical makeup of PEO and PTHF without additional fitting.[50] The model was extended to consider copolymer systems in which one monomer was more strongly adsorbed to the particle than the other; the monomer sequence was found to have a significant impact on the polymer adsorption.[56] Overall, there is broad agreement that the polymer-particle interaction strength is a crucial factor in determining the properties of the adsorbed polymer layer, that the adsorbed layer properties significantly affect the polymer dynamics, and that copolymer sequence affects polymer adsorption. However, a simulation study linking copolymer sequence to adsorption and therefore to the resulting dynamic properties is lacking.

With minor changes, this prior model is commensurate with polymers modeled in the standard Kremer-Grest manner.[47] The monomer-monomer interactions are given by the repulsive part of a Lennard-Jones (LJ) potential, as described above, and the strength of the interaction can be adjusted to account for unfavorable cross interactions between monomers. The particle-polymer interaction is an

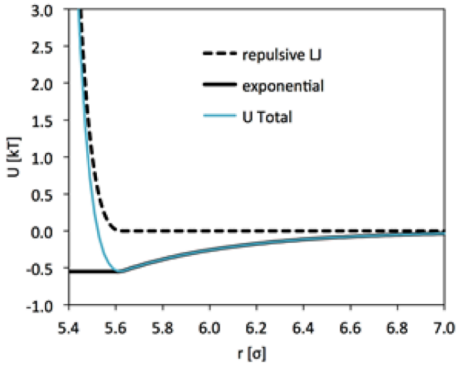

Figure 3: The nanoparticle-polymer pairwise interaction potential, blue, which is an exponential function coupled with a shifted repulsive LJ potential (as labeled). The parameters shown are nanoparticle size σ_{NP} = 10σ and strength of attraction $\varepsilon_{NP} = 0.55$kT, as in Ref [50].

exponential attraction as in the prior PRISM work[50,52-54] coupled with a shifted LJ repulsion[28,33]:

$$U_{NP}(r) = \begin{cases} 4\varepsilon\left[\left(\frac{\sigma}{r-\Delta}\right)^{12} - \left(\frac{\sigma}{r-\Delta}\right)^{6} + \frac{1}{4}\right] - \varepsilon_{NP} & ; \quad r \le \Delta + 2^{1/6}\sigma \\ -\varepsilon_{NP} e^{-(r-\Delta-2^{1/6}\sigma)/\alpha} & ; \quad r > \Delta + 2^{1/6}\sigma \end{cases}$$

where the shift factor $\Delta=(\sigma_{NP}-\sigma)/2$ as before, ε_{NP} is the strength of the interfacial attraction, and α=0.5 is the range of the attraction. Figure 3 shows a plot of this interaction potential.

Proposed Work and Preliminary Results

Effect of Polymer Adsorption

A snapshot of a preliminary simulation with monomer-naoparticle adsorption strength ε_{NP}=1 is shown in Figure 2 with adsorbed polymer highlighted. There is a visually apparent increased polymer density near the nanoparticle surface compared to the bulk. This is confirmed by the monomer-nanoparticle radial distribution function $g_{NP}(r)$ shown in Figure 3 ($g_{NP}(r)$ gives the probability of finding a monomer at a distance r given that there is a nanoparticle at the origin, normalized by the probability in the bulk). Note that even in the simulation with no added interfacial attraction, there is an increase in the local density of the polymer near the nanoparticle surface due to packing effects. The interfacial packing of monomers is expected to affect the local dynamics and thus the mechanical properties of the bulk composite.

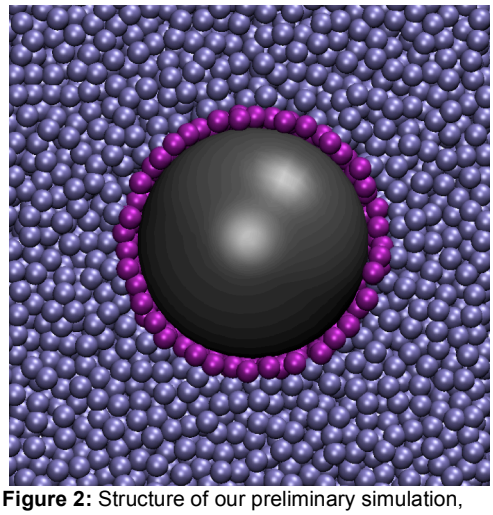

Figure 2: Structure of our preliminary simulation, with $\boldsymbol{\varepsilon_{NP}} = \mathbf{1}$. System consists of a single nanoparticle (black) surrounded by Kremer Grest polymer chains (blue-gray). A highly ordered, denser layer of adsorbed monomers can be seen near the nanoparticle surface (purple). In this context, monomers are defined as adsorbed if their centers are within $\boldsymbol{\Delta + 1.2\sigma}$ of the nanoparticle center. Figure shows a cut-away, cropped view of approximately half of the simulated system.

Further work will first focus on the structure and dynamics of the interfacial region surrounding a single nanoparticle at low volume fraction, as a function of the interaction strength with the monomers and copolymer structure. Specifically, monomers can be placed in a blocky ordered fashion, in a random fashion, or in a weighted random fashion to model the materials resulting from various synthesis processes. We will later consider higher volume fraction nanocomposites; however, we expect that it is intractable to simulate over the timescales required for particles of size 10 monomer diameters or larger to find their equilibrium state of agglomeration/dispersion. Instead of simulating such phenomena, we will instead fix particles in various random arrangements, and allow only the polymer to equilibrate around the known random nanoparticle structure. This allows us to address the scientific question of the effect of copolymer adsorption given that particles are randomly arranged, as is approximately the case in certain experimental systems. For long polymers that may be difficult to completely equilibrate using MD, Monte

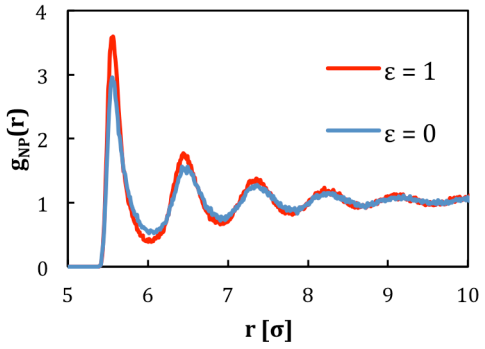

Figure 3: Monomer-nanoparticle radial distribution function from simulations with no interfacial attraction (blue) and with moderate interfacial attraction (red). Both show an increase in the local density of monomers around the nanoparticle due to packing effects, and the density is increased further when there is a nonzero interfacial attraction.

Carlo moves (using the double-bridging algorithm to allow chains to cross each other)[58] will also be used to ensure that even entangled polymers can fully equilibrate in a reasonable time.

We can calculate dynamic mechanical properties from equilibrium simulations using fluctuation dissipation relationships, for instance, to obtain the storage and loss modulus (often reported for experimental systems) across a broad frequency spectrum from the stress autocorrelation function.[36,59] However, long simulation times may be required to obtain good enough statistics to accurately show the storage and loss modulus from equilibrium simulations. Alternatively, mechanical properties can be calculated directly by non-equilibrium MD methods; for instance, viscosity as a function of shear rate can be calculated with good results by applying oscillatory shear to the simulated system.[37] We expect that experimental work in the Koelling group will yield rheology data as a function of nanoparticle loading for silica in polystyrene, silica in polybutadiene, and silica in a polystyrene-polybutadiene copolymer. However, it would be intractable to apply physically realistic shear rates across the full frequency spectrum that we expect the experimental work will analyze; instead we plan to simulate only a few frequencies of oscillation and attempt to reproduce the qualitative trends measured in the experimental samples. At these frequencies, we will also measure the full hysteresis loops, which can easily be created based on oscillatory response data[60] and existing analysis scripts can be modified for this purpose.[61] The will give us a more complete understanding of material hysteresis (including nonlinearities) which is critical to predicting traction and rolling resistance performance of tread compounds.

In addition to the nanocomposite systems, we will also simulate the bulk polymer so we can compare how adding nanoparticles affects storage and loss modulus and hysteresis versus the polymer melt. The size of the effect as a function of frequency found from the simulations will be compared to that measured experimentally. We will focus on the single nanoparticle simulations and low nanoparticle loading experiments to find appropriate values for the polymer-nanoparticle adsorption strengths. Other parameters such as the range of interaction and particle softness can be tuned if necessary to obtain good agreement. We will then be able to apply the same interaction parameters to the individual styrene and butadiene monomers in our simulations of copolymer systems, and will adjust the styrene-butadiene interactions as necessary to obtain good agreement.

With a validated model, we will explore in depth the underlying mechanisms behind the observed behaviors. Several quantities will be calculated as a function of distance from the nanoparticle, such as the end-to-end vector autocorrelation function.[28] Results from our

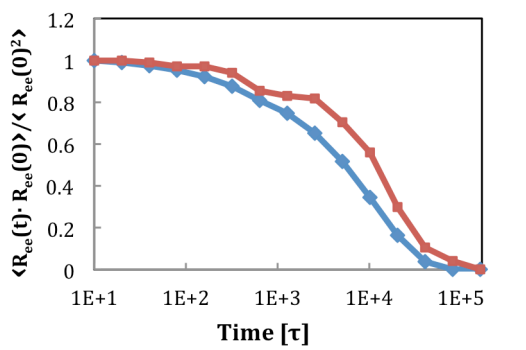

Figure 6: End-to-end autocorrelation function for polymers adsorbed to the nanoparticle at time 0 (red) compared to other polymers (blue).

preliminary simulations have already demonstrated a difference in this autocorrelation function for adsorbed polymers compared to those in the bulk, as shown in Figure 6. The relaxation of adsorbed chains initially appears similar to chains in the bulk, but after some time, the relaxation lags behind the bulk polymer. This observed slowdown in chain dynamics is expected to occur to a decreasing extent for polymers of increasing distance away from the nanoparticle surface. By measuring such quantities as a function of distance from the nanoparticle, we will be able to determine the width of the interfacial layer of adsorbed polymer with slowed dynamics as a function of interaction strength, nanoparticle loading, and copolymer configuration.

Effect of Grafting and Nanoparticle Arrangement

For the simplest version of the systems (all one type of monomer and fully repulsive interactions), we will also study the effect of using long polymers, polymers grafted to the particle surface, and high particle loadings. This will allow us to address how nanoparticles affect polymer entanglements and to understand the differences in mechanical behavior of the polymer melt around bare versus polymer-grafted nanoparticles. In systems with high grafting density and high particle loadings (little or no free polymer is present), the grafted polymer surrounds the particles evenly and particles can pack like pure hard spheres, forming an FCC structure. We are especially interested in how such a structure can affect entanglements between polymer chains grafted to particles. It is known that using high grafting densities promotes good particle dispersion, but high grafting density also creates a "brush" structure of polymers near the surface (due to steric constraints) that likely reduces entanglements. One question of interest is whether a system of long grafted chains but at relatively low grafting density could promote entanglements that would effectively hold particles together in a potentially optically active or mechanically robust close packed structure. For this part of the study, we will compare random and FCC arranged particles as a function of loading and in a polymer melt above the entanglement length. Both types of arrangements will be studied for bare and grafted systems; though we do not expect bare nanoparticles to arrange in an FCC structure experimentally, including such systems will allow us to tease apart the separate effects of grafting and nanoparticle packing arrangement that will both change upon grafting polymer to the particle surfaces. For all systems we will examine the number and location of entanglements of the polymers using a "primitive path" analysis.[63,66]

In preliminary calculations, dynamics of polymers around FCC-arranged bare nanoparticles were compared by analyzing their normal modes (or Rouse modes).[62,63] For a chain of length N and mode index p, the normal mode equation is given by

$$\boldsymbol{X}_p(t) \equiv \frac{1}{N}\sum_{i=1}^{N} \boldsymbol{r}_i(t)\cos\left[\frac{p\pi}{N}\left(i-\frac{1}{2}\right)\right] \qquad (5)$$

where the sum is over all monomers on the chain, $\boldsymbol{r}_i$ is the monomer position, and p is the mode. Mode $p = 0$ describes the motion of the chain center of mass and modes $p \geq 1$ describe the internal configurations of N/p sub-chain segments. The time autocorrelation of the normal modes $\langle \boldsymbol{X}_p(t) \cdot \boldsymbol{X}_p(0)\rangle / \langle {\boldsymbol{X}_p}^2(0)\rangle$, decays exponentially independent of the mode p for ideal chains,

$$\frac{\langle \boldsymbol{X}_p(t) \cdot \boldsymbol{X}_p(0) \rangle}{\langle \boldsymbol{X}_p{}^2(0) \rangle} = e^{-(\frac{t}{\tau_p})} \qquad (6)$$

where τ_p is the relaxation time, predicted by the Rouse model as $\tau_p{}^{-1} = 4W\sin^2(p\pi/2N)$. Here, $W = 3k_BT/\zeta b^2$ is the monomeric relaxation rate, a function of the statistical segment length b (Kuhn length), the monomeric friction coefficient ζ, and temperature. An important note when analyzing the normal modes of long entangled chains is that they only provide a useful comparison for chain relaxation in nanocomposites to pure homopolymer melts, and are not the modes in the ideal Rouse model.[64] Furthermore, for real polymer chains the autocorrelation can be better described by a stretched exponential function,[62,63]

$$\frac{\langle \boldsymbol{X}_p(t) \cdot \boldsymbol{X}_p(0) \rangle}{\langle \boldsymbol{X}_p{}^2(0) \rangle} = e^{-(\frac{t}{\tau_p{}^*})^{\beta_p}} \qquad (7)$$

where the relaxation time $\tau_p{}^*$ and the stretching parameter β_p both depend on chain length and mode index. The effective relaxation times can be calculated by integrating over the relaxation function with respect to time,

$$\tau_p^{\text{eff}} = \int_0^\infty e^{-(\frac{t}{\tau_p{}^*})^{\beta_p}} dt = \frac{\tau_p{}^*}{\beta_p} \Gamma(1/\beta_p) \qquad (8)$$

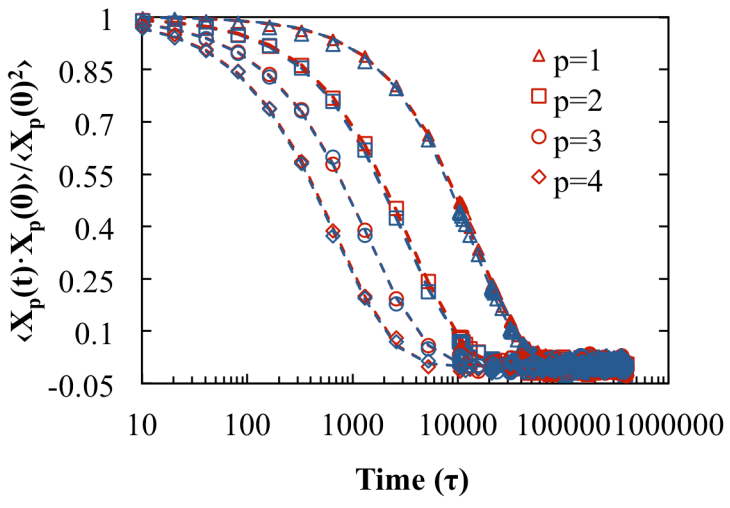

Figure 7: Normal mode autocorrelation function for polymers with N = 100 and FCC arranged nanoparticles (red) compared to pure melt homopolymer (blue).

where Γ() is the gamma function. Figures 7 and 8 show the autocorrelation functions for normal modes (p = 1-4) for two different chain lengths of polymers, N = 100 and N = 500, in a nanocomposite with nanoparticles arranged in an FCC lattice as seen in Figure 2. In Figures 7 and 8, we can see that the nanoparticles have little effect on chain relaxation for N = 100 and N = 500 at ϕ_{NP} = 0.2, which is in good agreement with other work at different nanoparticle sizes and moderately low volume fractions.[63-65] At higher volume fractions, however, chain dynamics slow due to the confinement induced by the nanoparticles.[63] The effective monomeric relaxation rate can be calculated by $W_p^{\text{eff}} = 1/4\tau_p^{\text{eff}}\sin^2(p\pi/2N)$ and can be seen in Figure 9 for both chain lengths. As noted earlier, the pure melt relaxation rate is about the same as the nanocomposite, thus confirming that the nanoparticles have little effect on chain relaxation at this volume fraction.

Further simulations are needed to compare the FCC arranged nanoparticle configuration to a random nanoparticle configuration. In addition, we will compare these systems to those with grafted nanoparticles at multiple grafting densities. For the grafted nanoparticle systems, we will

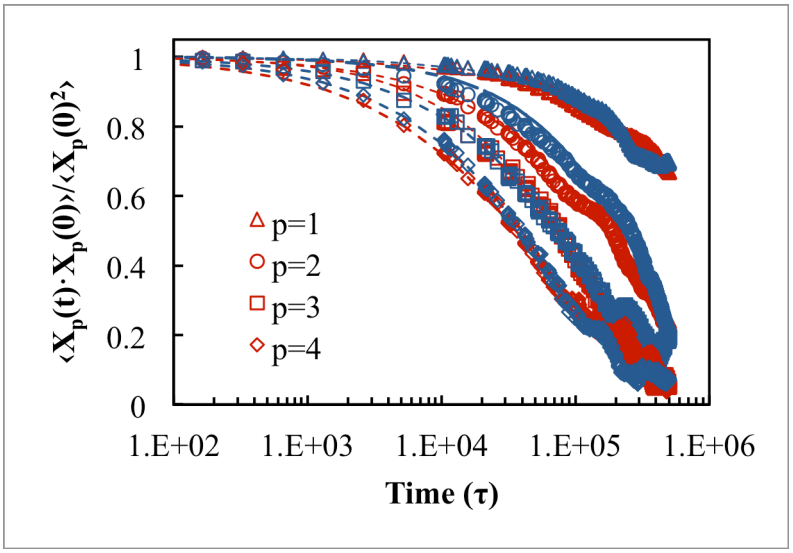

Figure 4: Normal mode autocorrelation function for polymers with *N* = 500 and FCC arranged nanoparticles (red) compared to pure melt homopolymer (blue).

separately analyze grafted and matrix chains, as these are expected to have significantly different properties. Similarly, the chains close to the nanoparticle surface may have slower relaxation rates with respect to the bulk polymers in an un-grafted nanoparticle system. To understand these differences, dynamical information such as end-to-end relaxation times will be calculated as a function of distance from the nearest nanoparticle as described for the adsorption study.

Summary

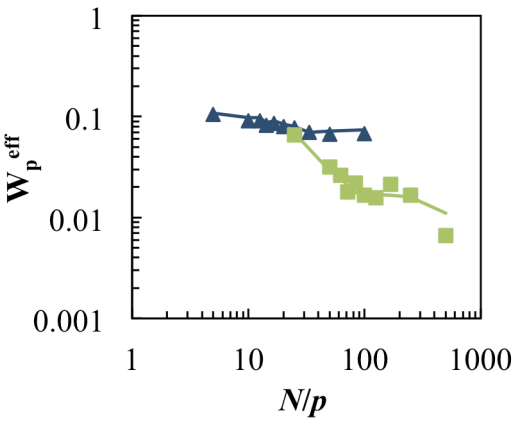

Figure 9: Effective monomeric relaxation rates for *N* = 100 (blue) and *N* = 500 (green) with FCC arranged nanoparticles. Straight lines are for the pure melt.

With the help of the Ohio Supercomputer Center (OSC), we will be able to simulate and gain insight into polymer nanocomposite systems. The effect of polymer adsorption and nanoparticle configuration is crucial in understanding PNCs, especially with high molecular weight (long chain) polymers. To study polymer adsorption, we will run simulations at different NP-monomer interactions and copolymer sequences. For the bare versus grafted nanoparticle systems, we will see the effect of grafting density and volume fraction on the entanglement network and dynamics of the polymer. This includes mechanical properties (such as loss and storage modulus) and dynamics of polymers near the particle surface compared to bulk. The information from these studies will advance the ability to rationally design new polymer nanocomposite materials which have a wide range of engineering applications.

REFERENCES

1. Bockstaller, M. R., et al. Block Copolymer Nanocomposites: Perspectives for Tailored Functional Materials. *Advanced Materials* **17**: 1331-1349 (2005).
2. Corbierre, M. K., et al. Polymer-Stabilized Gold Nanoparticles and Their Incorporation into Polymer Matrices. *American Chemical Society* **123**: 10411-10412 (2001).
3. Tanaka, T., et al. Polymer Nanocomposites as Dielectrics and Electrical Insulation-perspectives for Processing Technologies, Material Characterization and Future Applications. *IEEE Transactions on Dielectrics and Electrical Insulation* **11**(5): 763-784 (2004).
4. Paul, D. R. and L. M. Robeson Polymer nanotechnology: Nanocomposites. *Polymer* **49**(15): 3187-3204 (2008).
5. Payne, A. R. and Watson, W. F., Carbon Black Structure in Rubber. *Rubber Chem. Tech.* **36**, 147-155 (1963)
6. Grosch, K. A. The Relation Between the Friction and Viscoelastic Properties of Rubber. *Proc Royal Society of London*, Series A **274**, 21-39 (1964).
7. Grosch. K. A. The Rolling Resistance, Wear, and Traction Properties of Tread Compounds. *Rubber Chem. Tech.* **69**, 495-568 (1996).
8. Schallanmach, A. and Grosch, K. Tire Traction and Wear. *Mechanics of Pneumatic Tires 2nd Edition*, 365-474 (1981).
9. Rauline, R. Copolymer rubber composition with silica filler, tires having a base of said composition and method of preparing same. Patent US5227425 A (1993).
10. Pandey, Y. N., Papakonstantopoulos, G. J. and Doxastakis, M. Polymer/nanoparticle interactions: bridging the gap. *Macromolecules* **46**, 5097–5106 (2013).
11. Klüppel, M., La Gal, A., and Yang, X. Evaluation of sliding friction and contact mechanics of elastomers based on dynamic-mechanical analysis. *J. Chem. Phys.* **123**, 014704 (2005).
12. Kumar, S. K., and Krishnamoorti, R. Nanocomposites: Structure, Phase Behavior, and Properties. *Annual Rev. Chem. Biomol. Eng.* **1**, 37-58 (2010).
13. Sarvestani, A. S., and Picu C. R. Network model for the viscoelastic behavior of polymer nanocomposites. *Polymer* **45**, 7779-7790 (2004).
14. Dionne, P. J., Picu, C. R., and Ozisik, R. Adsorption and Desorption Dynamics of Linear Polymer Chains to Spherical Nanoparticles: A Monte Carlo Investigation. *Macromolecules* **39**, 3089-3092 (2006).
15. Kaewsakul, W., Sahakaro, K., Dierkes, W.K., and Noordermeer, J.W.M. Mechanistic aspects of silane coupling agents with different functionalities on reinforcement of silica-filled natural rubber compounds. *Polymer Eng. and Sci.* **55**. 836-842 (2015).
16. Bohm, G. A., Tomaszewski, W., Cole, W., and Hogan, T. Furthering the understanding of the non linear response of filler reinforced elastomers. *Polymer* **51,** 2057-2068 (2010).
17. Cichomski, E.M., Tolpekina, T.V., Schultz, S., Blume, A., Dierkes, W.K., and Noordermeer, J.W.M. Influence of silica-polymer bond microstructure on tire-performance indicators. *Kautschuk Herbst Kolloquium* **68**, 38-45 (2014).
18. Brinke, J. W. ten., Debnath, S. C., Reuvekamp, L. A. E. M., and Noordermeer, J.W.M., Mechanistic aspects of the role of coupling agents in silica–rubber composites. *Composites Sci. Tech.* **63**, 1165-1174 (2003).
19. Herd, C. et al. Use of surface-treated carbon blacks in an elastomer to reduce compound hysteresis and tire rolling resistance and improve wet traction. Patent WO2011028337 A2 (2011).
20. Fröhlich, J., Niedermeier, W., and Luginsland, H. The effect of filler-filler and filler-elastomer interaction on rubber reinforcement. *Composites: Part* A **36,** 449-460 (2005).
21. Sarvestani, A. S., and Jabbari, E. Modeling the Viscoelastic Response of Suspension of Particles in Polymer Solution: The Effect of Polymer-Particle Interactions. *Macromol. Theory Sim.* **16**, 378-385 (2007).

22. Kalathi, J. T., Grest, G. S., and Kumar, S. K. Universal Viscosity Behavior of Polymer Nanocomposites. *Phys. Rev. Lett.* **109**, 198301 (2012).
23. Maurel, G., Goujon, F., Schnell, B., and Malfreyt, P. Multiscale Modeling of the Polymer−Silica Surface Interaction: From Atomistic to Mesoscopic Simulations. *J. Phys Chem*. C **199**, 4817-4826 (2015).
24. Ndoro, T. V. M, Böhm, M. C., and Muller-Plathe, F. Interface and Interphase Dynamics of Polystyrene Chains Near Grafted and Ungrafted Silica Nanoparticles. *Macromolecules* **45**, 171−179 (2012).
25. Ghanbari, A., Ndoro, T. V., Leroy, F., Rahimi, M., C. Böhm, M., and Müller-Plathe, F. Interphase Structure in Silica-Polystyrene Nanocomposites: A Coarse-Grained Molecular Dynamics Study. *Macromolecules* **45**, 572−584 (2012).
26. Johnston, K. and Harmandaris, V. Hierarchical Simulations of Hybrid Polymer-Solid Materials. *Soft Matter* **9**, 6696−6710 (2013).
27. Johnston, K. and Harmandaris, V. Hierarchical Multiscale Modeling of Polymer-Solid Interfaces: Atomistic to Coarse-Grained Description and Structural and Conformational Properties of Polystyrene-Gold Systems. *Macromolecules* **46**, 5741−5750 (2013).
28. Li, Y., Kröger, M. and Liu, W. K. Nanoparticle effect on the dynamics of polymer chains and their entanglement network. *Phys. Rev. Lett.* **109**, 118001. (2012).
29. Li, Y., Kröger, M., and Liu, W. K. Nanoparticle Geometrical Effect on Structure, Dynamics and Anisotropic Viscosity of Polyethylene Nanocomposites. *Macromolecules* **45**, 2099−2112 (2012).
30. Picu, R. C. and Rakshit, A. Dynamics of free chains in polymer nanocomposites. *J. Chem. Phys.* **126**, 144909 (2007).
31. Starr, F. W., Schrøder, T. B., and Glotzer, S. C. Molecular dynamics simulation of a polymer melt with a nanoscopic particle. *Macromolecules* **35**, 4481–4492 (2002).
32. Starr, F. W. and Douglas, J. F. Modifying fragility and collective motion in polymer melts with nanoparticles. *Phys. Rev. Lett.* **106**, 115702 (2011).
33. Padmanabhan, V., Frischknecht, A. L., and Mackay, M. E. Effect of Chain Stiffness on Nanoparticle Segregation in Polymer/Nanoparticle Blends Near a Substrate. *Macromol. Theory Simul.* **21**, 98–105 (2012).
34. Voyiatzis, E., Rahimi, M., Müller-Plathe, F., and Böhm, M. C. How Thick Is the Polymer Interphase in Nanocomposites? Probing It by Local Stress Anisotropy and Gas Solubility. *Macromolecules* **47**, 7878–7889 (2014).
35. Smith, G. D., Bedrov, D., Li, L., and Byutner, O. A molecular dynamics simulation study of the viscoeleastic properties of polymer nanoomposites. *J. Chem. Phys.* **117**, 9478 (2002).
36. Sen, S., Thomin, J. D., Kumar, S. K., and Keblinski, P. Molecular Underpinnings of the Mechanical Reinforcement in Polymer Nanocomposites. *Macromolecules* **40,** 4059-4067 (2007).
37. Starr, F. W., Douglas, J. F., and Glotzer, S. C., Origin of Particle Clustering in a Simulated Polymer Nanocomposite and its Impact on Rheology. *J. Chem. Phys.* **119**, 1777 (2003).
38. Ganesan, V., Pryamitsyn, V., Surve, M., and Narayanan, B. Noncontinuum effects in nanoparticle dynamics in polymers. *J. Chem. Phys.* **124**, 221102 (2006).
39. Wang, M. and Hill, R. J. Anomalous bulk viscosity of polymer-nanocomposite melts. *Soft Matter* **5**, 3940-3953 (2009).
40. Akcora, P., et al. Anisotropic self-assembly of spherical polymer-grafted nanoparticles. *Nature Materials* **8**: 354-359 (2009).
41. Pryamtisyn, V., et al. Modeling the anisotropic self-assembly of spherical polymer-grafted nanoparticles. *J Chem Phys* **131**(22): 221102 (2009).
42. Mackay, M. E., et al. General Strategies for Nanoparticle Dispersion. *Science* **311**: 1740-1743 (2006).
43. Green, P. F. The structure of chain end-grafted nanoparticle/homopolymer nanocomposites. *Soft Matter* **7**(18): 7914 (2011).
44. Chevigny, C., et al. Polymer-Grafted-Nanoparticles Nanocomposites: Dispersion, Grafted Chain Conformation, and Rheological Behavior. *Macromolecules* **44**(1): 122-133 (2011).

45. Shen, J., et al. Molecular dynamics simulations of the structural, mechanical and visco-elastic properties of polymer nanocomposites filled with grafted nanoparticles. *Physical Chemistry Chemical Physics* **17**(11): 7196-7207 (2015).
46. Shen, J., et al. Revisiting the dispersion mechanism of grafted nanoparticles in polymer matrix: a detailed molecular dynamics simulation. *Langmuir* **27**(24): 15213-15222 (2011).
47. Kremer, K. and G. S. Grest Dynamics of entangled linear polymer melts: A molecular-dynamics simulation. *J Chem Phys* **92**(8): 5057 (1990).
48. Weeks, J. D. Role of Repulsive Forces in Determining the Equilibrium Structure of Simple Liquids. *J Chem Phys* **54**(12): 5237 (1971).
49. Allen, M. P., & Tildesley, D. J. Computer simulation of liquids. *Oxford university press* (1989).
50. Hall, L. M., Anderson, B. J., Zukoski, C. F., and Schweizer, K. S. Concentration fluctuations, local order and the collective structure of polymer nanocomposites. *Macromolecules* **42**, 8435–8442 (2009).
51. Anderson, B. J. and Zukoski, C. F. Rheology and microstructure of an unentangled polymer nanocomposite melt. *Macromolecules* **41**, 9326–9334 (2008).
52. Hooper, J. B. and Schweizer, K. S. Real space structure and scattering patterns of model polymer nanocomposites. *Macromolecules* **40**, 6998–7008 (2007).
53. Kim, S. Y., Hall, L. M., Schweizer, K. S., and Zukoski, C.F. Long wavelength concentration fluctuations and cage scale ordering of nanoparticles in concentrated polymer solutions. *Macromolecules* **43**, 10123–10131 (2010).
54. Kim, S.Y. and Zukoski, C.F. Role of polymer segment-particle surface interactions in controlling nanoparticle dispersions in concentrated polymer solutions. *Langmuir* **27**, 10455–10463 (2011).
55. Hooper, J. B., Schweizer, K. S., Desai, T. G., Koshy, R. and Keblinski, P. Structure, surface excess and effective interactions in polymer nanocomposite melts and concentrated solutions. *J. Chem. Phys.* **121**, 6986–6997 (2004).
56. Hall, L. M. and Schweizer, K. S. Impact of Monomer Sequence, Composition and Chemical Heterogeneity on Copolymer-Mediated Effective Interactions between Nanoparticles in Melts, *Macromolecules* **44**, 3149-3160 (2011).
57. Shinoda, W., et al. Rapid estimation of elastic constants by molecular dynamics simulation under constant stress. *Physical Review B* **69**(13) (2004).
58. Auhl, R., Everaers, R., Grest, G. S., Kremer, K. and Plimpton, S. J. Equilibration of long chain polymer melts in computer simulations. *J. Chem. Phys.* **119**, 12718–12728 (2003).
59. Sen, S., Kumar, S. K., and Keblinski, P. Viscoelastic Properties of Polymer Melts from Equilibrium Molecular Dynamics Simulations. *Macromolecules* **38**, 650-653 (2005).
60. Falk, M. L. and Langer J. S. Dynamics of viscoplastic deformation in amorphous solids. *Physical Review E* **57,** 7192 (1998).
61. Brown, J. R. and McCoy, J. D. Nonlinear dynamic heat capacity of a bead-spring polymeric glass former. *J. Chem. Phys.* **137,** 244504 (2012).
62. Shaffer, J. S. (1994). Effects of chain topology on polymer dynamics: Bulk melts. *J. Chem. Phys.*, *101*(5), 4205–4213. http://doi.org/10.1063/1.467470
63. Li, Y., Kroger, M., & Liu, W. K. Nanoparticle effect on the dynamics of polymer chains and their entanglement network. *Physical Review Letters*, *109*(11), 1–5 (2012).
64. Kalathi, J. T., Kumar, S. K., Rubinstein, M., & Grest, G. S. Rouse mode analysis of chain relaxation in polymer nanocomposites. *Macromolecules*, *47*(19), 6925–6931 (2014).
65. Li, Y., Kröger, M., & Liu, W. K. Dynamic structure of unentangled polymer chains in the vicinity of non-attractive nanoparticles. *Soft Matter*, *10*(11), 1723–37 (2014).
66. Karatrantos, A., Clarke, N., Composto, R. J., & Winey, K. I. Structure, entanglements and dynamics of polymer nanocomposites containing spherical nanoparticles. *IOP Conference Series: Materials Science and Engineering*, *64*, (2014).
67. Plimpton, S. J. Fast Parallel Algorithms for Short-Range Molecular Dynamics. *Journal of Computational Physics* **117**(1): 1-19 (1995).